

Identification of the Essential Catalytic Residues and Selectivity-Related Residues of Maltooligosyltrehalose Trehalohydrolase from the Thermophilic Archaeon *Sulfolobus solfataricus* ATCC 35092

TSUEI-YUN FANG,^{*,†} WEN-CHI TSENG,[‡] TONG-YUAN SHIH,[†] AND
MEI-YING WANG[†]

Department of Food Science, National Taiwan Ocean University, Keelung, Taiwan, and Department of Chemical Engineering, National Taiwan University of Science and Technology, Taipei, Taiwan

Maltooligosyltrehalose trehalohydrolase (MTHase) catalyzes the release of trehalose by cleaving the α -1,4-glycosidic linkage next to the α -1,1-linked terminal disaccharide of maltooligosyltrehalose. Mutations at residues D255, E286, and D380 were constructed to identify the essential catalytic residues of MTHase, while mutations at residues W218, A259, Y328, F355, and R356 were constructed to identify selectivity-related residues of the enzyme. The specific activities of the purified D255A, E286A, and D380A MTHases were only 0.15, 0.09 and 0.01%, respectively, of that of wild-type MTHase, suggesting that these three residues are essential catalytic residues. Compared with wild-type MTHase, A259S, Y328F, F355Y, and R356K MTHases had increased selectivity ratios, which were defined as the ratios of the catalytic efficiencies for glucose formation to those for trehalose formation in the hydrolysis of maltooligosaccharides and maltooligosyltrehaloses, respectively, while W218A and W218F MTHases had decreased selectivity ratios. When starch digestion was carried out at 75 °C and wild-type and mutant MTHases were, respectively, used with isoamylase and maltooligosyltrehalose synthase (MTSase), the ratios of initial rates of glucose formation to those of trehalose formation were inversely correlated to the peak trehalose yields.

KEYWORDS: Maltooligosyltrehalose trehalohydrolase; selectivity; mutation; trehalose; substrate specificity; starch; *Sulfolobus*

INTRODUCTION

Maltooligosyltrehalose trehalohydrolase (EC 3.2.1.141, MTHase, also known as glycosyltrehalose trehalohydrolase, glycosyltrehalose-hydrolyzing enzyme, and trehalose-forming enzyme) mainly catalyzes the release of trehalose by cleaving the α -1,4-glycosidic linkage next to the α -1,1-linked terminal disaccharide of maltooligosyltrehalose. Trehalose (α -D-glucopyranosyl- α -D-glucopyranoside) is a nonreducing sugar formed from two glucose (G₁) units joined by an α -1,1 linkage. The sugar has a remarkable ability to protect proteins and membranes from dryness, heat, and osmotic changes and has been approved as a novel food ingredient under the GRAS terms in the United States and the European Union (1, 2). It is gaining more applications in many different areas, such as a sweetener component, a preservative or stabilizer for food, cosmetics, vaccines, medicines, cells, and organs (2). Trehalose can be

produced from starch by thermophilic maltooligosyltrehalose synthase (MTSase) and MTHase combined with a debranching enzyme. However, both MTSase and MTHase catalyze a side hydrolysis reaction that would decrease the yield of trehalose (3–5). This suggests that engineering the selectivity of both MTSase and MTHase to decrease the side hydrolysis reactions would increase the trehalose yield. Our previous study also showed that F405Y MTSase, which had a decreased reaction of the side hydrolysis, had resulted in a higher yield of trehalose production from starch when it replaced wild-type MTSase (6, 7).

MTHase from *Sulfolobus solfataricus* KM1 contains three major domains (A, C, and E) and two subdomains (B and D), of which domain A is the (β/α)₈ barrel catalytic domain with B and D subdomains as insertions into this barrel (8). According to the information from CAZY, a Web resource on glycosyl hydrolases at <http://afmb.cnrs-mrs.fr/CAZY/>, MTHase has been previously classified in family 13 of glycosyl hydrolases. The sequence and structural analysis suggested that domain A contains three catalytic residues (Asp252, Glu283, and Asp377) that are conserved in family 13 of glycosyl hydrolases (8). Asp252 and Glu283 likely act as the catalytic base and acid,

* Corresponding author. Telephone: 886-2-2462-2192, ext. 5141. Fax: 886-2-2462-2586. E-mail: tyfang@mail.ntou.edu.tw.

[†] National Taiwan Ocean University.

[‡] National Taiwan University of Science and Technology.

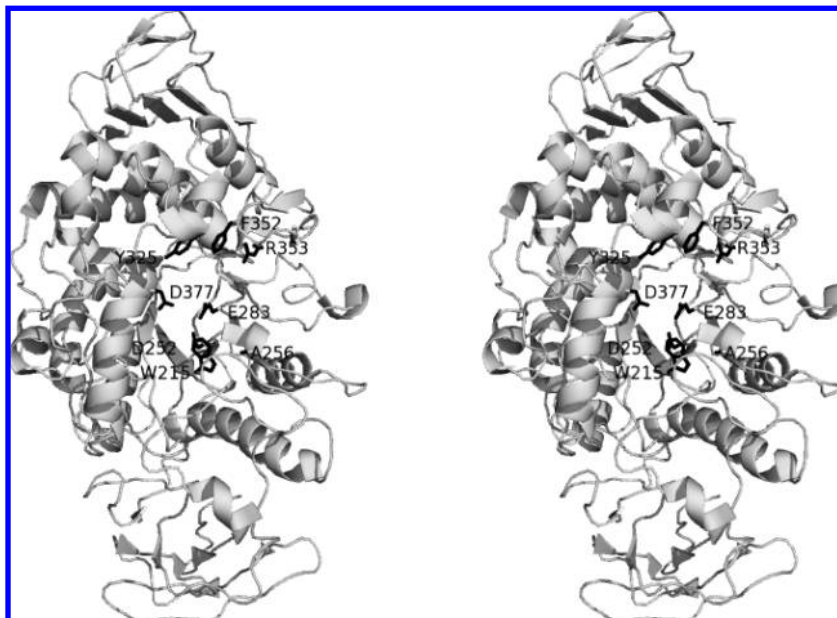


Figure 1. Stereoview of the MTHase monomer from *S. solfataricus* KM1 (8), illustrating the active site. Residues W215, D255, A256, E283, Y325, F352, R353, and D377 in *S. solfataricus* KM1 MTHase are equivalent to residues W218, D255, A259, E286, Y328, F355, R356, and D380 in *S. solfataricus* ATCC 35092 MTHase. The figure was prepared with PyMOL (9).

respectively (8). **Figure 1** shows the stereoview of the MTHase monomer from *S. solfataricus* KM1, illustrating the active site (8, 9). The crystal structures of MTHase from *S. solfataricus* KM1 also suggested that W215 is likely an important substrate binding residue (8). The structure comparisons between the MTHase from *S. solfataricus* KM1 and other several family 13 glycosidases also suggested that the trehalose end of maltooligosyltrehaloses binds subsites +1 and +2, which are located near the C-terminal side of the catalytic barrel, to provide a recognition for the trehalose moiety, and subsite +2 is the most critical region for substrate discrimination between maltooligosyltrehaloses and maltooligosaccharides (8). The residues Y325, F352, and R353, which are located at the C-terminal side of the catalytic barrel, might form a steric barrier at subsite +2 of the substrate binding cleft (8). In addition, when we compared the four conserved regions in the active sites of MTHases from five different strains of the *Sulfolobus* genus, we found that four MTHases have Ala but only *Sulfolobus shibatae* B12 has Ser corresponding to position 259 of MTHase of *S. solfataricus* ATCC 35092, which is in the third conserved region and usually a residue important for specificity (10, 11). However, no mutation analysis has been carried out to identify these catalytic and selectivity-related residues of MTHase.

The MTHase from *S. solfataricus* ATCC 35092, also known as P2, has been purified and characterized in our previous study (10). In this study, site-directed mutagenesis was used to construct various individual mutations in this enzyme to identify the essential catalytic residues and selectivity-related residues. To find the relationships between trehalose yield and specific parameters, we not only investigated the kinetic parameters of the wild-type and mutant enzymes but also carried out the production of trehalose from the digestion of 10% (w/v) soluble starch at 75 °C by using wild-type and mutant MTHases, respectively, along with isoamylase and MTSase.

MATERIALS AND METHODS

Materials. *Escherichia coli* Rosetta (DE3) was from Novagen. QuickChange XL site-directed mutagenesis kit was purchased from Stratagene. G₁, maltopentaose (G₅), maltohexaose (G₆), maltoheptaose (G₇), glucoamylase, 3,5-dinitrosalicylic acid (DNS), and bovine serum

albumin (BSA) were supplied by Sigma. Q-Sepharose, sephacryl S-200 HR, and protein low molecular weight standards were from Amersham Pharmacia Biotech. Microcon centrifugal filter unit was obtained from Millipore.

Site-Directed Mutagenesis. The MTHase gene in the previously constructed vector pET-15b- Δ H-*treZ* (10) was mutated by polymerase chain reaction according to the instructions of the QuickChange XL site-directed mutagenesis kit as previously described (6). The designed mutations were included in the mutagenic primers which have 27–41 bases individually.

Production and Purification of MTHase. Wild-type and mutant MTHases were produced by culturing pET-15b- Δ H-*treZ*-transformed *E. coli* BL21-CodonPlus (DE3)-RIL at 37 °C in Terrific broth medium supplemented with 100 μ g/mL of ampicillin plus 34 μ g/mL of chloramphenicol as previously described (10). The wild-type and mutant MTHases were purified after cell disruption by using heat treatment, streptomycin sulfate precipitation, and Q-Sepharose anion exchange column chromatography as previously described (10). The molecular weights of both wild-type and mutant MTHases were determined using a BioSep-SEC-S4000 gel filtration column as previously described (10). Protein concentration was quantitated by Bradford's method (12) with BSA as standards.

Preparation of Maltooligosyltrehaloses. Maltotriosyltrehalose (G₃T), maltotetraosyltrehalose (G₄T), and maltopentaosyltrehalose (G₅T) were prepared as previously described (10).

Enzyme Activity Assay. The MTHase activity was assayed at 60 °C for 10 min by using 2.8 mM G₄T as substrate in 0.05 M citrate phosphate buffer (pH 5), and the activity of the enzyme was determined by the DNS assay in our previous study (10). One unit (U) of MTHase activity was defined as the amount of enzyme required to produce 1 μ mol of trehalose in one minute. The specific activity was defined as the amount of enzyme activity/mg of the enzyme (U/mg). The effects of pH and temperature on the activity and stabilities of wild-type and mutant MTHases were also determined according to the methods previously described (10).

Enzyme Kinetics. The initial rates for hydrolysis of G₃T–G₅T and G₅–G₇ were determined at 60 °C in 50 mM citrate phosphate buffer at pH 5 by using 8–10 substrate concentrations ranging from 2 to 50 mM as previously described (9). The values of k_{cat} , K_M , and k_{cat}/K_M were calculated by fitting the initial rates as a function of substrate concentration to the Michaelis–Menten equation using Enzfitter software (Elsevier-Biosoft). The standard errors of these parameters were obtained from the fitting results. The change of transition-state

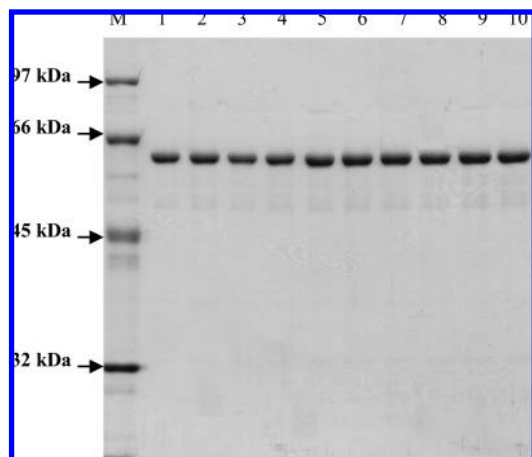


Figure 2. SDS-PAGE of the purified wild-type and mutant MTHases. A 10% minigel was stained with Coomassie Brilliant Blue R-250. Lane M: molecular weight standards; lanes 1–10: wild-type, D255A, E286A, D380A, A259S, Y328F, W218A, W218F, F355Y, and R356K MTHases, respectively.

binding energy $[\Delta(\Delta G)]$ for substrate hydrolysis caused by the mutation was used to estimate the binding strength of the substrate in the transition-state complex and was calculated by the equation $\Delta(\Delta G) = -RT \ln[(k_{cat}/K_M)_{mut}/(k_{cat}/K_M)_{wt}]$, where the subscripts mut and wt denote mutant and wild-type enzymes, respectively (13). The selectivity ratio was calculated as $[k_{cat}/K_M(G_n)]/[k_{cat}/K_M(G_{n-2}T)]$.

Production of Trehalose from Starch. In an effort to produce trehalose from starch, purified thermophilic isoamylase, MTSase, and MTHase were used concurrently. The purified thermophilic isoamylase and MTSase were prepared according to the method described in our previous studies (6, 14). The reaction was carried out at 75 °C with 10% (w/v) soluble starch in a 50 mM citrate phosphate buffer of pH 5. The enzyme concentration was 0.063 μ M for both wild-type and mutant MTHases. Aliquots of 800 U/g-starch of isoamylase and 40 U/g-starch of MTSase were also added to the reaction mixture. The samples were taken at 10, 20, 30, 40, and 50 min to determine the initial rates and were also taken at 2, 4, 6, 8, 12, 18, and 24 h to determine the trehalose yield. The formations of G_1 were determined by a glucose oxidase method as previously described (7). For the detection of trehalose, glucoamylase was added to hydrolyze the residual starch, maltooligosaccharides and maltooligosyltrehalose, and then the reaction mixtures were filtered and analyzed by HPLC as previously described (7). The initial rates of trehalose and G_1 formation were calculated by fitting experimental data obtained within 1 h to the equation $c = At + B$, where c is the product concentration, t is the time and A (the initial rate) and B are constants obtained by linear regression as previously described (7). Peak trehalose yield was the average of the three highest consecutive trehalose yield measurements, which were sampled at 12, 18, and 24 h in this study.

RESULTS

Purity and Characteristics of Wild-Type and Mutant MTHases. The purity of the enzyme was analyzed by sodium dodecyl sulfate-polyacrylamide gel (SDS-PAGE; 10% minigel) according to the method of Laemmli (15). The purity of wild-type and mutant MTHases was very good, as indicated by SDS-PAGE (Figure 2). Since the wild-type MTHase is a homodimer (10), the molecular masses of the purified wild-type and mutant MTHases under nonreducing conditions were analyzed by HPLC using a BioSep-S4000 gel filtration column as previously described (10). The molecular masses of HPLC analysis showed that all mutant MTHases are homodimers and have a molecular weight around 129 kDa.

The specific activities of mutant MTHases were in general lower than that of wild-type MTHase (Table 1). The specific

Table 1. Specific Activities of the Wild-Type and Mutant MTHases for Hydrolysis of G_4T at 60 °C in 50 mM Citrate Phosphate Buffer, pH 5^a

MTHase form	specific activity (U/mg)
wild-type	814 ± 20
W218A	5.31 ± 0.11
W218F	52.0 ± 3.3
D255A	1.23 ± 0.11
A259S	787 ± 18
E286A	0.74 ± 0.04
Y328F	492 ± 20
F355Y	597 ± 16
R356K	472 ± 8
D380A	0.10 ± 0.01

^a One unit (U) of MTHase activity was defined as the amount of enzyme required to produce 1 μ mol of trehalose in one minute. The specific activity was defined as the amount of enzyme activity/mg of the enzyme (U/mg). Data represent the mean ± SD from triplicate experiments.

activities of D255A, E286A, and D380A MTHases were only 0.15, 0.09, and 0.01%, respectively, of that of wild-type. The severe losses in activity indicate that D255, E286, and D380 are catalytic residues.

Wild-type and W218A, W218F, A259S, Y328F, F355Y, and R356K MTHases had optimal activities at pH 5 and 85 °C (data not shown). After a two-hour incubation at 80 °C, wild-type and those six mutant MTHases retained virtually all of their activities (data not shown). The good thermostability of these enzymes suggested the purified mutant MTHases were well folded without any long-range conformational changes that may be a consequence of mutation.

Enzyme Kinetics. Kinetic parameters (k_{cat} and K_M) for the hydrolysis of G_3T-G_5T and G_5-G_7 at 60 °C and pH 5 are given in Table 2. The catalytic efficiencies (k_{cat}/K_M) for G_4T and G_6 hydrolysis of W218A MTHase were 0.97 and 0.62%, respectively, of those of wild-type MTHase, while those of W218F MTHase were 4.1 and 0.62%, respectively, of those of wild-type MTHase. The low specific activities (Table 1) and catalytic efficiencies (Table 2) of these two mutant enzymes might prevent their applications in an industrial process to produce trehalose from starch, and therefore we did not carry out further the kinetic studies by using other forms of substrates and the trehalose production from starch.

By comparison with wild-type MTHase, A259S MTHase had slightly lower catalytic efficiencies for hydrolysis of G_3T-G_5T and similar catalytic efficiencies for hydrolysis of G_5 and G_6 , while a slightly higher catalytic efficiency for hydrolysis of G_7 . Y328F MTHase had 40–73 and 76–84% catalytic efficiencies of those of wild-type for hydrolysis of G_3T-G_5T and G_5-G_7 , respectively. F355Y MTHase had somewhat lower catalytic efficiencies for hydrolysis of G_3T-G_5T and slightly lower catalytic efficiencies for hydrolysis of G_5 and G_7 , while a slightly higher catalytic efficiency for hydrolysis of G_6 . R356K MTHase had 45–59 and 101–130% catalytic efficiencies of those of wild-type for hydrolysis of G_3T-G_5T and G_5-G_7 , respectively.

Production of Trehalose from Starch. The digestion of 10% (w/v) soluble starch was used to study the yield of trehalose production by wild-type, A259S, Y328F, F355Y, and R356K MTHases along with isoamylase and MTSase at both a high reaction temperature and a high substrate concentration. All of the reactions reached more than 80% trehalose yield in 6 h, and the yield almost reached equilibrium in 12 h (data not shown). The G_1 formation in the starch digestion was also determined because of the side reactions to release G_1 from maltooligosaccharides also catalyzed by both MTHase and

Table 2. Kinetic Parameters of the Wild-Type and Mutant MTHases for Hydrolysis of G₃T–G₅T and G₅–G₇ at 60 °C in 50 mM Citrate Phosphate Buffer, pH 5^a

TFE form	trehalose formation			G ₁ formation		
	G ₃ T	G ₄ T	G ₅ T	G ₅	G ₆	G ₇
Wild-Type						
k_{cat} (s ⁻¹)	1030 ± 28 ^b	1192 ± 34	1226 ± 36	17.7 ± 0.5	18.2 ± 0.7	6.01 ± 0.13
K_M (mM)	7.22 ± 0.48	5.66 ± 0.37	5.89 ± 0.45	5.86 ± 0.40	5.63 ± 0.51	2.63 ± 0.20
k_{cat}/K_M (s ⁻¹ mM ⁻¹)	143 ± 6	210 ± 8	198 ± 9	3.02 ± 0.13	3.24 ± 0.22	2.29 ± 0.13
selectivity ratio ^c (×10 ²)	2.12	1.54	1.16			
W218A						
k_{cat} (s ⁻¹)		16.0 ± 0.5			0.36 ± 0.01	
K_M (mM)		7.91 ± 0.61			20.5 ± 1.7	
k_{cat}/K_M (s ⁻¹ mM ⁻¹)		2.03 ± 0.09			0.02 ± 0.00	
selectivity ratio (×10 ²)		0.99				
$\Delta(\Delta G)^d$ (kJ/mol)		12.8			14.4	
W218F						
k_{cat} (s ⁻¹)		58.4 ± 2.4			0.54 ± 0.02	
K_M (mM)		6.79 ± 0.54			23.2 ± 1.6	
k_{cat}/K_M (s ⁻¹ mM ⁻¹)		8.59 ± 0.64			0.02 ± 0.00	
selectivity ratio (×10 ²)		0.23				
$\Delta(\Delta G)$ (kJ/mol)		8.86			13.7	
A259S						
k_{cat} (s ⁻¹)	1002 ± 29	1106 ± 60	1282 ± 31	17.4 ± 0.6	13.5 ± 0.6	6.49 ± 0.24
K_M (mM)	8.55 ± 0.65	6.79 ± 0.52	7.15 ± 0.42	5.37 ± 0.48	4.69 ± 0.44	2.19 ± 0.25
k_{cat}/K_M (s ⁻¹ mM ⁻¹)	117 ± 5	163 ± 14	179 ± 7	3.24 ± 0.18	2.89 ± 0.16	2.97 ± 0.25
selectivity ratio (×10 ²)	2.76	1.77	1.60			
$\Delta(\Delta G)$ (kJ/mol)	0.55	0.71	0.27	-0.19	0.32	-0.63
Y328F						
k_{cat} (s ⁻¹)	634 ± 26	654 ± 22	760 ± 34	14.4 ± 0.6	8.23 ± 0.28	5.00 ± 0.13
K_M (mM)	10.9 ± 0.9	5.03 ± 0.45	5.26 ± 0.42	5.82 ± 0.57	3.01 ± 0.28	2.88 ± 0.20
k_{cat}/K_M (s ⁻¹ mM ⁻¹)	57.8 ± 2.6	130 ± 8	144 ± 11	2.47 ± 0.14	2.73 ± 0.17	1.73 ± 0.08
selectivity ratio (×10 ²)	4.27	2.10	1.20			
$\Delta(\Delta G)$ (kJ/mol)	2.50	1.33	0.87	0.56	0.47	0.77
F355Y						
k_{cat} (s ⁻¹)	734 ± 25	721 ± 30	741 ± 29	19.1 ± 0.7	9.50 ± 0.28	5.49 ± 0.17
K_M (mM)	13.6 ± 1.0	6.94 ± 0.64	5.81 ± 0.44	7.74 ± 0.58	2.16 ± 0.20	2.81 ± 0.25
k_{cat}/K_M (s ⁻¹ mM ⁻¹)	54.1 ± 2.4	104 ± 5	127 ± 10	2.47 ± 0.10	4.39 ± 0.30	1.95 ± 0.12
selectivity ratio (×10 ²)	4.57	4.24	1.53			
$\Delta(\Delta G)$ (kJ/mol)	2.69	1.96	1.22	0.56	-0.85	0.44
R356K						
k_{cat} (s ⁻¹)	572 ± 23	627 ± 24	675 ± 26	15.5 ± 0.6	12.6 ± 0.3	6.49 ± 0.24
K_M (mM)	8.90 ± 0.74	6.73 ± 0.65	5.75 ± 0.45	5.08 ± 0.43	3.42 ± 0.22	2.19 ± 0.25
k_{cat}/K_M (s ⁻¹ mM ⁻¹)	64.2 ± 3.8	93.7 ± 5.8	117 ± 9	3.06 ± 0.16	3.68 ± 0.15	2.97 ± 0.25
selectivity ratio (×10 ²)	4.77	3.93	2.53			
$\Delta(\Delta G)$ (kJ/mol)	2.21	1.53	1.44	-0.037	-0.36	-0.72

^a The degrees of polymerization of G₃T, G₄T, and G₅T were equal to those of G₅, G₆, and G₇, which were 5, 6, and 7, respectively. ^b Standard error. ^c Selectivity ratio: $[k_{cat}/K_M(G_n)]/[k_{cat}/K_M(G_{n-2})]$. ^d Change of transition-state energy: $\Delta(\Delta G) = -RT \ln[(k_{cat}/K_M)_{mut}/(k_{cat}/K_M)_{wt}]$ (13).

MTSase. The initial rates of trehalose and G₁ formation in the starch digestion and their ratios were also obtained. Ratios of the initial rates of G₁ formation to trehalose formation were calculated to evaluate the selectivity for G₁ formation versus that of trehalose formation. **Figure 3** shows the relationship between peak trehalose yields (the average of the three highest consecutive trehalose yield measurements that were sampled at 12, 18, and 24 h in this study) and the ratios of initial rates of G₁ formation to those of trehalose formation. All tested mutant MTHases, including A259S, Y328F, F355Y, and R356K MTHases, had higher ratios of initial rates of G₁ formation to trehalose formation compared with that of wild-type MTHase (**Figure 3**). Peak trehalose yields and ratios of initial rates of G₁ formation to those of trehalose formation were inversely correlated (**Figure 3**). Therefore, the lower ratios of the initial rate of G₁ formation to that of trehalose formation from the starch digestion will result in the higher trehalose yield.

MTHase Selectivity toward G₅–G₇ Hydrolysis versus G₃T–G₅T Hydrolysis. Selectivity ratios were calculated from the kinetic parameters of wild-type and mutant MTHases for hydrolysis of G₃T–G₅T and G₅–G₇ as given in **Table 2**. The selectivity ratio is expressed as the ratio of catalytic efficiency

of G_n hydrolysis over that of G_(n-2)T hydrolysis. W218A and W218F MTHases had decreased selectivity ratios compared to that of wild-type MTHase, whereas A259S, Y328F, F355Y, and R356K MTHases had increased selectivity ratios.

Figure 4 depicts the relationships between peak trehalose yield from starch digestion and the selectivity ratios from kinetic studies for wild-type and A259S, Y328F, F355Y, and R356K MTHases. Only the selectivity ratios obtained from the hydrolysis of G₃T and G₅ were inversely correlated to peak trehalose yields. When Y328F MTHase was not included, the selectivity ratios obtained from the hydrolysis of G₄T and G₆ were also inversely correlated to peak trehalose yields.

DISCUSSION

In a previous study, we had investigated the effects of MTSase mutations on trehalose yield by using 10% (w/v) soluble starch as substrate and by combining isoamylase and MTHase in the reaction mixture. We found that the ratios of the initial rate of G₁ formation to that of trehalose formation from the starch digestion provide a better prediction for high trehalose yield. In addition, mutant MTSases with decreased

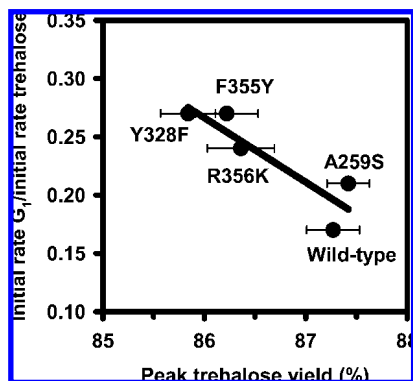


Figure 3. Relationship between peak trehalose yields and (initial rate of G_1 formation/initial rate of trehalose formation) during the digestion of 10% (w/v) soluble starch at 75 °C in 50 mM citrate phosphate buffer (pH 5) using the wild-type and mutant MTHases along with isoamylase and MTSase. The peak trehalose yield was represented by mean \pm SD from three highest consecutive trehalose yield measurements, which were sampled at 12, 18, and 24 h in this study.

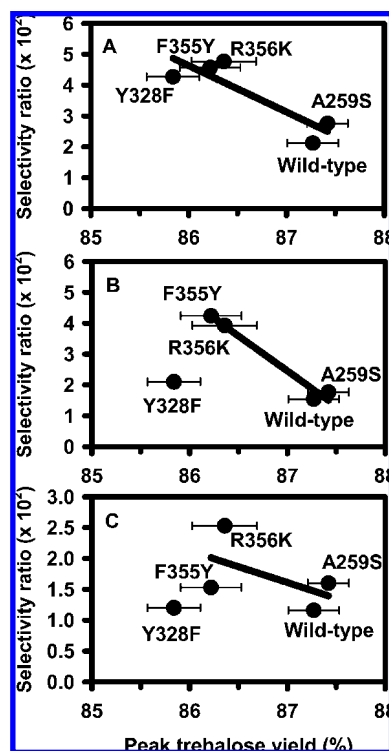


Figure 4. Relationships between the peak trehalose yields from starch digestion and the selectivity ratios from kinetic studies by the wild-type and mutant MTHases. (A) Selectivity ratios for G_5 hydrolysis over G_3T hydrolysis. (B) Selectivity ratios for G_6 hydrolysis over G_4T hydrolysis. (C) Selectivity ratios for G_7 hydrolysis over G_5T hydrolysis. The peak trehalose yield was represented by mean \pm SD as in Figure 3.

selectivity ratios for hydrolysis over transglycosylation had a higher peak trehalose yield except for one mutant MTSase. In this study, we investigated the effects of MTHase mutations on trehalose yield also by using 10% (w/v) soluble starch as substrate and by combining isoamylase and MTSase in the reaction mixture. Since the peak trehalose yields and ratios of initial rates of G_1 formation to those of trehalose formation were inversely correlated (Figure 3), we confirmed that the lower ratios of the initial rate of G_1 formation to that of trehalose formation from the starch digestion could predict the higher trehalose yield. In addition, the MTHases with lower selectivity

ratios obtained from the hydrolysis of G_3T and G_5 had a higher peak trehalose yield.

Residues D255, E286, and D380, which are equivalent to the proposed catalytic residues D252, E283, and D377 of MTHase from *S. solfataricus* KM1, respectively (8), were mutated to alanine to identify their roles as catalytic residues. The almost complete loss of specific activities confirmed that they are catalytic residues. Residue W218, which is equivalent to residue W215 of MTHase from *S. solfataricus* KM1, was mutated to Ala and Phe to identify its importance in substrate binding. Tryptophan is the most common residue involved in hydrophobic interactions in protein–carbohydrate complexes, and W215 of MTHase from *S. solfataricus* KM1 was proposed to make substantial contacts with bound substrate (8). We calculated the transition-state energy to estimate the binding strength of the enzyme–substrate complex in the transition state. As some earlier studies pointed out, the change of transition-state energy, $\Delta(\Delta G)$, associated with the loss of a hydrogen bond between uncharged groups on the substrate and enzyme is between 2.1 and 6.3 kJ/mol, while that for the loss of a hydrogen bond between an uncharged group on the substrate and a charged group on the enzyme is between 14.6 and 18.8 kJ/mol (7, 16). The large changes in $\Delta(\Delta G)$ for G_4T and G_6 hydrolysis by W218A MTHase, 12.8 and 14.4 kJ/mol, respectively, and those by W218F MTHase, 8.86 and 13.7 kJ/mol, respectively (Table 2), are approximate to the loss of two uncharged hydrogen bonds between enzyme and the substrate in the transition state. In addition, the atom NE1 of Trp is both a hydrogen acceptor and hydrogen donor, and, therefore, Trp residue has the ability to form two hydrogen bonds with the substrate. These results suggested that there might be two hydrogen bonds between substrate and residue W218 on the wild-type MTHase of *S. solfataricus* ATCC 35092. The G_4T can occupy the subsites +2, +1, -1, -2, -3, and -4, and G_6 can occupy the subsites +1, -2, -3, -4, and -5. Therefore, the losses of hydrogen bond caused by mutations on W218 presumably occurred between subsites +1 to -4 but not on subsite +2. Residue W218 in *S. solfataricus* ATCC 35092 MTHase is equivalent to residue W241 in *Deinococcus radiodurans* MTHase (DrMTHase). The crystal structure of the DrMTHase–trehalose complex also suggested that W241 can hydrogen bond directly to the sugar ring of the substrate (17). In addition, the hydrophobic interactions also play a role in the substrate binding when we compared kinetic parameters and $\Delta(\Delta G)$ values for G_4T hydrolysis obtained from W218A and W218F MTHases.

Residue A259 in *S. solfataricus* ATCC 35092 MTHase is equivalent to residue S257 in *S. shibatae* B12 (10). This residue is located in the third highly conserved region and usually important for specificity. Mutation A259S was designed to create a decreased hydrophobic interaction, possibly forming hydrogen bonds between the enzyme and substrate. A259S MTHase had slightly increased selectivity ratios compared to those of wild-type MTHase. However, the small change of $\Delta(\Delta G)$ values, from -0.63 to 0.71 kJ/mol, indicated that this mutation had only minor effects on the transition-state substrate binding.

Residues Y328, F355, and R356 in *S. solfataricus* ATCC 35092 MTHases are equivalent to residues Y325, F352, and R353, respectively, in *S. solfataricus* KM1 MTHase (Figure 1). Those residues probably form a steric barrier at subsite +2 of the substrate binding cleft (8). Mutations Y328F, F355Y, and R356K were designed to create minor changes in this steric barrier. The small change of $\Delta(\Delta G)$ values, from -0.85 to 2.69 kJ/mol, indicated that these mutations had only minor effects

on transition-state substrate binding. However, Y328F, F355Y, and R356K MTHases had moderately increased selectivity ratios compared to those of wild-type MTHase. These minor changes near the subsite +2 substantially changed the selectivity of MTHase especially when the degree of polymerization of substrate was decreased.

In conclusion, in this study we confirmed the catalytic roles of D255, E286, and D380 and suggested the existence of two hydrogen bonds between substrate and the enzyme at position W218. In addition, the minor changes in the substrate binding strength at residues A259, Y328, F355, and R356 can alter the selectivity of MTHase. The lower ratios of the initial rate of G₁ formation to that of trehalose formation from the digestion of soluble starch predict high trehalose yield.

ABBREVIATIONS USED

MTSase, maltooligosyltrehalose synthase; MTHase, maltooligosyltrehalose trehalohydrolase; *S. solfataricus*, *Sulfolobus solfataricus*; *S. shibatae*, *Sulfolobus shibatae*; G₁, glucose; G₅, maltopentaose; G₆, maltohexaose; G₇, maltoheptaose; G₃T, maltotriosyltrehalose; G₄T, maltotetraosyltrehalose; G₅T, maltopentaosyltrehalose; DNS, 3,5-dinitrosalicylic acid; BSA, bovine serum albumin; Δ(ΔG), change of transition-state energy; SDS-PAGE, sodium dodecyl sulfate-polyacrylamide gel electrophoresis.

LITERATURE CITED

- (1) Crowe, J. H. Trehalose as a "chemical chaperone": Fact and fantasy. *Adv. Exp. Med. Biol.* **2007**, *594*, 143–158.
- (2) Richards, A. B.; Krakowka, S.; Dexter, L. B.; Schmid, H.; Wolterbeek, A. P.; Waalkens-Berendsen, D. H.; Shigoyuki, A.; Kurimoto, M. Trehalose: A review of properties, history of use and human tolerance, and results of multiple safety studies. *Food Chem. Toxicol.* **2002**, *40*, 871–898.
- (3) Kato, M. Trehalose production with a new enzymatic system from *Sulfolobus solfataricus* KM1. *J. Mol. Catal. B: Enzym.* **1999**, *6*, 223–233.
- (4) Kobayashi, K.; Komeda, T.; Miura, Y.; Kettoku, M.; Kato, M. Production of trehalose from starch by novel trehalose-producing enzymes from *Sulfolobus solfataricus* KM1. *J. Ferment. Bioeng.* **1997**, *83*, 296–298.
- (5) Mukai, K.; Tabuchi, A.; Nakada, T.; Shibuya, T.; Chaen, H.; Fukuda, S.; Kurimoto, M.; Tsujisaka, Y. Production of trehalose from starch by thermostable enzymes from *Sulfolobus acidocaldarius*. *Starch/Staerke* **1997**, *49*, 26–30.
- (6) Fang, T. Y.; Tseng, W. C.; Chung, Y. T.; Pan, C. H. Mutations on aromatic residues of the active site to alter selectivity of the

Sulfolobus solfataricus maltooligosyltrehalose synthase. *J. Agric. Food Chem.* **2006**, *54*, 3585–3590.

- (7) Fang, T. Y.; Tseng, W. C.; Pan, C. H.; Chung, Y. T.; Wang, M. Y. Protein engineering of *Sulfolobus solfataricus* maltooligosyltrehalose synthase to alter its selectivity. *J. Agric. Food Chem.* **2007**, *55*, 5588–5594.
- (8) Feese, M. D.; Kato, Y.; Tamada, T.; Kato, M.; Komeda, T.; Miura, Y.; Hirose, M.; Hondo, K.; Kobayashi, K.; Kuroki, R. Crystal structure of glycosyltrehalose trehalohydrolase from the hyperthermophilic archaeum *Sulfolobus solfataricus*. *J. Mol. Biol.* **2000**, *301*, 451–464.
- (9) DeLano, W. L. *The PyMOL Molecular Graphics System*; DeLano Scientific: Palo Alto, CA, 2002. <http://www.pymol.org>.
- (10) Fang, T. Y.; Tseng, W. C.; Guo, M. S.; Shih, T. Y.; Hung, X. G. Expression, purification, and characterization of the maltooligosyltrehalose trehalohydrolase from the thermophilic archaeon *Sulfolobus solfataricus* ATCC 35092. *J. Agric. Food Chem.* **2006**, *54*, 7105–7112.
- (11) MacGregor, E. A.; Janecek, S.; Svensson, B. Relationship of sequence and structure to specificity in the α-amylase family of enzymes. *Biochim. Biophys. Acta* **2001**, *1546*, 1–20.
- (12) Bradford, M. M. A rapid and sensitive method for the quantitation of microgram quantities of protein utilizing the principle of protein-dye binding. *Anal. Biochem.* **1976**, *72*, 248–254.
- (13) Wilkinson, A. J.; Fersht, A. R.; Blow, D. M.; Winter, G. Site-directed mutagenesis as a probe of enzyme structure and catalysis: Tyrosyl-tRNA synthetase cysteine-35 to glycine-35 mutation. *Biochemistry* **1983**, *22*, 3581–3586.
- (14) Fang, T. Y.; Tseng, W. C.; Yu, C. J.; Shih, T. Y. Characterization of the thermophilic isoamylase from the thermophilic archaeon *Sulfolobus solfataricus* ATCC 35092. *J. Mol. Catal. B: Enzym.* **2005**, *33*, 99–107.
- (15) Laemmli, U. K. Cleavage of structural proteins during the assembly of the head of bacteriophage T4. *Nature* **1970**, *227*, 680–685.
- (16) Fersht, A. R.; Shi, J. P.; Knill-Jones, J.; Lowe, D. M.; Wilkinson, A. J.; Blow, D. M.; Brick, P.; Carter, P.; Waye, M. M.; Winter, G. Hydrogen bonding and biological specificity analysed by protein engineering. *Nature* **1985**, *314*, 235–238.
- (17) Timmins, J.; Leiros, H. K.; Leonard, G.; Leiros, I.; McSweeney, S. Crystal structure of maltooligosyltrehalose trehalohydrolase from *Deinococcus radiodurans* in complex with disaccharides. *J. Mol. Biol.* **2005**, *347*, 949–963.

Received for review November 13, 2007. Revised manuscript received March 10, 2008. Accepted April 10, 2008. This work was supported by the Center for Marine Bioscience and Biotechnology at the National Taiwan Ocean University and Grant NSC-95-2313-B-019-021-MY2 from the National Science Council at Taiwan.

JF073320B